

# FINITE ELEMENT METHODS WITH COORDINATE CHARTS FOR SOLVING ELLIPTIC EQUATIONS ON MANIFOLDS

LIZHEN QIN <sup>\*</sup>, SHANGYOU ZHANG <sup>†</sup>, AND ZHIMIN ZHANG <sup>‡</sup>

**Abstract.** We apply finite element methods to elliptic problems on compact Riemannian manifolds. The elliptic equation on manifolds is reduced to coupled equations on Euclidean spaces by coordinate charts. The advantage of this strategy is to avoid global triangulations on curved manifolds in the finite element method. The resulting finite element problem can be solved globally, or locally by nonoverlapping or overlapping domain decomposition methods. The method is illustrated by a 4D problem. We present the theory and computational results.

**AMS subject classifications.** Primary 65N30; Secondary 46E25, 20C20

**Key words.** Riemannian manifolds, elliptic problems, domain decomposition methods, finite element methods

**1. Introduction.** Elliptic problems on Riemannian manifolds are important both in analysis and in geometry (see [35, 20]). The so called geometric partial differential equations appear in many areas, such as multifluid dynamics, micromagnetics, and image processing, cf. [2, 3, 12, 13, 33, 38, 34]. A simple example is the surface Laplace equation

$$-\Delta_S u = 0. \tag{1.1}$$

Here  $\Delta_S$  is the Laplace-Beltrami operator, defined on an  $n$ -dimensional manifold  $M$ . When solving such a surface elliptic equation by the finite element method, a challenge is the construction of a grid on the manifold (a surface grid), cf. [7, 8, 12, 28, 37]. We propose a different approach that coordinate charts are introduced in the weak form of the surface Laplace equation:

$$\int_M \nabla_S u \nabla_S v dM = \sum_k \int_{\Omega_k} g_k^{\alpha\beta} \tilde{u}_{x_\alpha} \tilde{v}_{x_\beta} dx \quad \forall v \in H^1(\Omega_k). \tag{1.2}$$

Here  $g_k^{\alpha\beta}$  is the metric matrix of coordinate  $F_k : \Omega_k \rightarrow M_k$ ,  $M_k \cap M_{k'} = \emptyset$  and  $\cup M_k = M$ . Then the finite element method is applied inside each Euclidean domain  $\Omega_k \subset \mathbb{R}^n$ . The novelty of this approach is to avoid manifold grids by solving the corresponding differential equations on Euclidean spaces.

After taking coordinates of the manifolds and reducing (1.1) to (1.2), we can easily adopt high order finite elements and/or uniform grids, to achieve high-order accuracy and superconvergence much easier, compared with those done currently on surface grids [7, 8, 12, 37]. It is even worse in implementation, if one constructs a manifold grid for  $C^1$  elements [26], in addition to theoretical difficulty in analysis.

When the piecewise local coordinate charts in (1.2) are non-overlapping and  $C^1$  continuous across the boundary, the resulting elliptic equations on Euclidean spaces can be separated to nonoverlapping subdomains. In this case the resulting finite element equations can be solved globally by a direct method, such as the conjugate

---

<sup>\*</sup>Department of Mathematics, Wayne State University, Detroit, MI 48202. qinlz@hotmail.com.

<sup>†</sup>Department of Mathematical Sciences, University of Delaware, Newark, DE 18716. szhang@udel.edu.

<sup>‡</sup>Department of Mathematics, Wayne State University, Detroit, MI 48202. ag7791@wayne.edu.

gradient method or the multigrid method. Or the finite element equations can be solved locally by the nonoverlapping domain decomposition method. The Optimized Schwarz Nonoverlapping method [25, 29, 9, 10, 15, 16, 29, 30] can be easily implemented. The same idea appeared in [11] to compute a global conformal map by the nonoverlapping domain decomposition method. Slightly different from the domain decomposition on a flat Euclidean space, the metric matrices  $g_k^{\alpha,\beta}$  are same on the inter-boundary of submanifolds,  $\partial M_k \cap \partial M_{k'}$ .

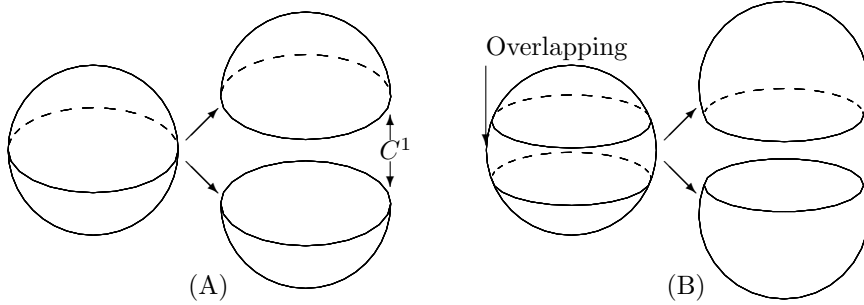


FIG. 1.1. Nonoverlapping (left) and overlapping local charts.

As  $C^1$  nonoverlapping charts may not be easily constructed in general (cf. Figure 1.1), we also consider overlapping charts in (1.2). Then (1.2) leads to an overdetermined, but consistent variational problem, i.e., the solution  $u(y)$  appears in more than one equation. Unless the coordinates in different subdomains are identical on the overlapping region, the resulting finite element equations could be no longer consistent. However, we could restrict the finite element grid lines of one subdomain  $\Omega_k$  coincide with the boundaries of other overlapping domains  $\Omega_{k'}$ . Here we assume the charts are appropriate so that the grid line of boundary  $\Omega_{k'}$  is mapped to some grid lines of  $\Omega_k$  in the sense,  $F_{k'}(T_{k',i}^{(n-1)}) \in \{F_k(T_{k,j}^{(n-1)})\}$  where  $T_i^{(n-1)}$  is a  $(n-1)$ -dimensional simplex on the boundary of  $\Omega_{k'}$ . Then the finite element equations are consistent, without any projection/interpolation involved. That is, the finite element solution is multiply defined in the interior of overlapped regions  $M_k \cap M_{k'}$ , but uniquely defined on nonoverlapping region  $M_k \setminus \cup_{k' \neq k} M_{k'}$ . Thus, the finite element equations can be solved globally, or by the overlapping domain decomposition method. We can take off the boundary grid matching restriction. Then we do not have a global finite element set of equations, instead we have to use the overlapping domain decomposition method where a boundary interpolation is required to match solutions on nonmatching grids. This is different from traditional overlapping domain decomposition method where the overlapping subdomains can easily have same grids. This is, our case is similar to an overlapping domain decomposition problem where overlapping grids are different (see [23, 24, 31, 39]).

We choose a Laplace problem on a 3-dimensional manifolds for the numerical test. The method is to be generalized to solving the Einstein's equations, where the space derivatives are computed on a manifold in a 4-dimensional time-space, cf. [1, 21, 41]. It is very difficult to construct hypersurface tetrahedral grids in  $R^4$ . In both of our methods, nonoverlapping and overlapping methods, we avoid surface grids in  $R^{n+1}$  (on an  $n$ -manifold  $M$ ) and boundary surface grids in  $R^n$  (on the boundary of  $M_i$ ). To our knowledge, such a tetrahedral grid on a surface in 4D is not done anywhere, for the finite element method.

The outline of this paper is as follows. Section 2 presents a model problem and its variational form. Section 3 defines the finite element method and shows the convergence of the finite element method. Some numerical results are presented in Section 4.

**2. A model problem and its two variational problem.** For fixing the idea, we consider the following elliptic model problem on an  $n$ -dimensional compact orientable smooth Riemannian manifold  $M$  with  $\partial M = \emptyset$ .

$$-\Delta_S u + bu = f, \quad (2.1)$$

where  $\Delta_S$  is the Laplace-Beltrami operator,  $b > 0$  is a constant. We need to address two issues about (2.1). First, in contrast to a usual elliptic problem on a domain of  $R^n$ , (2.1) has no boundary condition. If  $\partial M \neq \emptyset$ , it is necessary to impose some boundary conditions. Second, in contrast to the usual Laplace operator in  $R^n$ ,  $\sum_{\alpha=1}^n \frac{\partial^2}{\partial x_\alpha^2}$ , the Laplace operator  $\Delta_S$  on  $M$  *cannot* be expressed by *coordinates globally* because  $M$  does not have a global coordinate in general. Locally, we can choose a coordinate chart  $(x_1, \dots, x_n)$  for  $M$ . In this particular coordinate chart, the Riemannian metric tensor is expressed as

$$g = \sum_{\alpha, \beta=1}^n g_{\alpha\beta} dx_\alpha \otimes dx_\beta,$$

where the matrix  $(g_{\alpha\beta})_{n \times n}$  is symmetric and positive definite. The Laplace operator is as follows,

$$\Delta_S u = \frac{1}{\sqrt{G}} \sum_{\alpha=1}^n \frac{\partial}{\partial x_\alpha} \left( \sum_{\beta=1}^n g^{\alpha\beta} \sqrt{G} \frac{\partial u}{\partial x_\beta} \right),$$

where  $G = \det((g_{\alpha\beta})_{n \times n})$  is the determinant of the matrix  $(g_{\alpha\beta})_{n \times n}$  and  $(g^{\alpha\beta})_{n \times n}$  is the inverse of  $(g_{\alpha\beta})_{n \times n}$ .

In order to translate (2.1) into an equivalent variational problem, we need the volume form and Green Formula on an oriented Riemannian manifold with boundary. Locally, we can define the volume form as  $\sqrt{G} dx_1 \wedge \dots \wedge dx_n$ , and

$$\nabla_S u = \sum_{\alpha, \beta=1}^n g^{\alpha\beta} \frac{\partial u}{\partial x_\alpha} \frac{\partial}{\partial x_\beta}$$

as the gradient of  $u$ . If  $v$  is another function, we can compute the inner product,

$$\langle \nabla_S u, \nabla_S v \rangle = \sum_{\alpha, \beta=1}^n g^{\alpha\beta} \frac{\partial u}{\partial x_\alpha} \frac{\partial v}{\partial x_\beta}.$$

Then we can consider the Riemannian integral  $\int_M \Delta_S u$  and  $\int_M \langle \nabla_S u, \nabla_S v \rangle$  on  $M$ . In general, if  $f$  is a function, we can consider its Riemannian integral on  $M$ . Locally, in some open subset  $\Omega_k$ , it is an integral

$$\int_{\Omega_k} f(x_1, \dots, x_n) \sqrt{G} dx_1 \wedge \dots \wedge dx_n = \int_{\Omega_k} f(x_1, \dots, x_n) \sqrt{G} dx_1 \cdots dx_n,$$

where the right hand of the above equality is a multiple integral over a domain in  $R^n$ . Now we have the following Green Formula.

**THEOREM 2.1** (Green Formula). *If  $M$  is a compact orientable Riemannian manifold,  $u, v \in C^\infty(M)$ , then we have*

$$\int_M -\Delta_S u \cdot v = \int_M \langle \nabla_S u, \nabla_S v \rangle - \int_{\partial M} \frac{\partial_S u}{\partial \mathbf{n}} v,$$

where  $\mathbf{n}$  is the outward normal vector on  $\partial M$ , and  $\frac{\partial_S u}{\partial \mathbf{n}} = \langle \nabla u, \mathbf{n} \rangle$  the outward normal derivative.

Just like the the situation of  $R^n$ , we can also define distributions on  $M$  which are called *currents* (see [32, 19]). Hence Theorem 2.1 can be extended to the case of functions with weak derivatives. We can change (2.1) to a variational form. Since we assume  $\partial M = \emptyset$  for (2.1), we have  $\int_{\partial M} \frac{\partial u}{\partial n} = 0$ . Thus we get

$$\int_M \langle \nabla_S u, \nabla_S v \rangle + \int_M b u v = \int_M f v \quad \forall v \in C^\infty(M).$$

However, this global description without coordinates (see [20]) cannot be used in computation. The coordinates-free description is convenient for the theoretical analysis. After choosing coordinate charts for  $M$ , we would get a variational form with boundary integrals. Depending on if such charts are overlapping or not, we have two different variational forms.

Let  $\{\varphi_i\}$  be a  $C^1$  nonoverlapping set of coordinate charts on  $M$ . That is, there is a finite set of mappings  $\varphi_i$  such that

$$\begin{aligned} \varphi_i &: \Omega_i \rightarrow M_i, \quad \varphi_i \in C^1(\Omega_i), \quad \Omega_i \subset R^n, \\ M_i \cap M_j &= \emptyset, \quad i \neq j, \quad M = \text{interior}(\cup_i \overline{M_i}), \\ \frac{\partial \varphi_i^{-1}}{\partial \mathbf{n}_i} &= -\frac{\partial \varphi_j^{-1}}{\partial \mathbf{n}_j} \quad \text{on interface } \gamma_{ij} = \partial M_i \cap \partial M_j, \end{aligned} \quad (2.2)$$

where  $\mathbf{n}_i$  is the unit out normal to  $M_i$ , and  $\gamma_{ij}$  is an  $(n-1)$ -dimensional, smooth manifold.

We note that we require  $\varphi_i$  be continuously differentiable across the boundary so that the boundary integral in the variational form would be cancelled. But this can be done only for few special manifolds such as  $n$ -sphere or  $n$ -torus or their smooth perturbations. In general, the coordinate charts might not be made  $C^1$  across nonoverlapping subdomain boundary on  $M$ . In this case we would use overlapping charts to cover  $M$ , which leads an overlapping domain decomposition.

Next is the equivalence theorem under nonoverlapping  $C^1$  charts.

**THEOREM 2.2.** *Let  $\{\varphi_i\}$  be a  $C^1$  nonoverlapping set of coordinate charts on  $M$ , defined in (2.2). The solution  $u((\varphi_i)^{-1}(\mathbf{y}))$  of (2.1) is the unique solution of the following variational problem, find  $u(\mathbf{x}) \in \{\oplus H^1(\Omega_i) \mid u((\varphi_i^{-1}(\mathbf{x})) \in H^1(M)\}$  such that*

$$\sum_i \int_{\Omega_i} \left( \sum_{\alpha, \beta=1}^n g_i^{\alpha\beta} \frac{\partial u}{\partial x_\alpha} \frac{\partial v}{\partial x_\beta} + b u v - f v \right) \sqrt{G^{(i)}} d\mathbf{x} = 0 \quad (2.3)$$

for all  $v(\mathbf{x}) \in (\oplus H^1(\Omega_i))$ . Here  $H^1(\Omega_i)$  is the Sobolev space on a Euclidean domain  $\Omega_i$ .

*Proof.* Applying the Green formula, Theorem 2.1, on the boundary of each sub-domain, we have  $v((\varphi_i^{-1}(\mathbf{y}))$  glued together as a global  $H^1(M)$  function, and we have an cancellation of boundary integrals, as

$$\int_{\gamma_{ij,x}} \sum_{\alpha,\beta=1}^n g_i^{\alpha\beta} \frac{\partial u}{\partial x_\alpha} n_\beta v d\gamma_x = - \int_{\gamma_{ji,x}} \sum_{\alpha,\beta=1}^n g_j^{\alpha\beta} \frac{\partial u}{\partial x_\alpha} n_{i,\beta} v d\gamma_x,$$

where  $\gamma_{ij,x} = \{\mathbf{x} \in \bar{\Omega}_i \mid \varphi_i(\mathbf{x}) \in \gamma_{ij}\}$  and  $\gamma_{ji,x} = \{\mathbf{x} \in \bar{\Omega}_j \mid \varphi_j(\mathbf{x}) \in \gamma_{ij}\}$ . Again, we note that this posts a strong requirement on the coordinate charts  $\{\varphi_i\}$ , i.e.,  $\varphi_i^{-1}$  and  $\varphi_j^{-1}$  are  $C^1$  across  $\gamma_{ij}$  and  $\gamma_{ij}$  is a smooth ( $C^1$ ) manifold of  $(n-1)$  dimension.  $\square$

As nonoverlapping  $C^1$  coordinate charts (2.2) may not be possible in general, we introduce next overlapping coordinate charts. The purpose is to avoid all integrals and grids on curved boundary as well as on curved surface. The overlapping charts are still restrictive. Let  $\{\varphi_i\}$  be an overlapping set of coordinate charts on  $M$  (cf. the right figure in Figure 1.1):

$$\begin{aligned} \varphi_i : \Omega_i &\rightarrow M_i, \quad \varphi_i \in C^1(\Omega_i), \quad \Omega_i \subset R^n, \\ M &= \text{interior}(\cup_i M_i). \end{aligned} \quad (2.4)$$

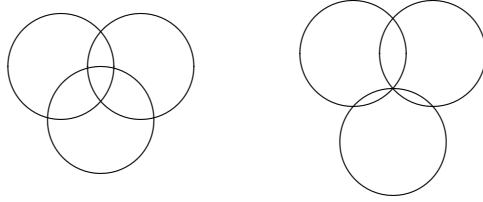


FIG. 2.1. An overlapping (left) and not an overlapping set of charts.

**THEOREM 2.3.** *Let  $\{\varphi_i\}$  be an overlapping set of coordinate charts on  $M$ , defined in (2.4). The solution  $u(\varphi_i^{-1}(\mathbf{y}))$  of (2.1) is the unique solution of the following variational problem, find  $u(\mathbf{x}) \in \oplus H^1(\Omega_i)$  such that*

$$\begin{aligned} \int_{\Omega_i} \left( \sum_{\alpha,\beta=1}^n g_i^{\alpha\beta} \frac{\partial u}{\partial x_\alpha} \frac{\partial v}{\partial x_\beta} + buv - fv \right) \sqrt{G^{(i)}} d\mathbf{x} = 0 \quad \forall v(\mathbf{x}) \in H_0^1(\Omega_i), \\ \text{and } u|_{\Omega_i}(\mathbf{x}_i) = u|_{\Omega_j}(\mathbf{x}_j) \quad \text{if } \varphi_i(\mathbf{x}_i) = \varphi_j(\mathbf{x}_j). \end{aligned} \quad (2.5)$$

Here  $H_0^1(\Omega_i)$  is the Sobolev space on a Euclidean domain  $\Omega_i$  with 0 trace.

*Proof.* Applying the Green formula, Theorem 2.1, on each sub-manifold  $M_i$ , as  $v(\varphi_i^{-1}(\mathbf{y})) \in H_0^1(M_i)$ , the solution  $u$  of (2.1) satisfies (2.5). If (2.5) has two solutions  $u_1$  and  $u_2$ , then  $u = u_1 - u_2$  satisfies the homogeneous equation:

$$\int_{\Omega_i} \left( \sum_{\alpha,\beta=1}^n g_i^{\alpha\beta} \frac{\partial u}{\partial x_\alpha} \frac{\partial v}{\partial x_\beta} + buv \right) \sqrt{G^{(i)}} d\mathbf{x} = 0 \quad \forall v \in H_0^1(\Omega_i).$$

In particular, its maximum  $u(\mathbf{y}_0) = \max u(M)$  is achieved within a sub-manifold  $M_i$ . Note that every point of  $M$  is inside some  $M_i$ . Thus, by Hopt theorem [18], a generalized maximum principle of Gauss (cf. [17], 1838),  $u \equiv u(\mathbf{y}_0)$  on  $M_i$ , and consequently  $u \equiv u(\mathbf{y}_0)$  on whole  $M$ . The one-domain variational problem leads to  $bu = 0$ . Thus  $u(\mathbf{y}_0) = 0$ . In the same fashion, we derive  $u = \min u(M) = 0$  as  $-u$  satisfies the above homogeneous equation too. We remark that  $u$  is uniquely defined, on the overlapping region  $M_i \cap M_j$  too.  $\square$

**3. The finite element method in Euclidean space.** We use Euclidean coordinates in the finite element method, to solve (2.1). Let  $M$  be a  $n$ -dimensional oriented Riemannian manifold. We partition  $M$  into overlapping or nonoverlapping submanifolds,  $M_i (i = 1, \dots, K)$ . Let coordinate charts  $\{\varphi_i : \Omega_i \rightarrow M_i\}$  be defined either in (2.2) or (2.4). Let  $\mathcal{T}_{(i),h}$  be an  $n$ -dimensional triangulation on  $\Omega_i$ :

$$\mathcal{T}_{(i),h} = \{T \mid T \text{ is an } n\text{-dimensional, nondegenerate simplex,} \\ \cup T \approx \Omega_i, \text{ diam}T \leq h\}.$$

Here a triangulation means that the intersection of any two simplices  $T_1$  and  $T_2$ , is a lower dimensional, face simplex of both simplices, or an empty set, cf. [6]. For the nonoverlapping charts (2.2), the boundary of  $\Omega_i$  is usually curved. In this case, if we use  $P_1$  elements in (3.2),  $\partial(\cup T)$  approximates  $\partial\Omega_i$  to  $O(h^2)$ , which ensures the optimal approximation of the finite element solution. But if we use higher order finite elements in (3.2),  $T$  would be an  $n$ -dimensional simplex with one curved face. This is the standard isoparametric finite element [4, 6], i.e., the finite element reference mapping (not an affine mapping) is a degree  $k$  polynomial, the same order polynomial of the finite element space itself. In both cases of nonoverlapping and overlapping coordinate charts, we require a triangulation matching on the interface and the overlapping region (for overlapping charts):

$$\mathcal{T}_h = \{\cup \mathcal{T}_{(i),h} \mid \varphi_i(T_{i,f}) = \varphi_j(T_{j,f_2}) \text{ for some } T_j \in \mathcal{T}_{(j),h} \text{ if} \\ \varphi_i(T_{i,f}) \subset M_j\}, \quad (3.1)$$

where  $T_{i,f}$  is either the  $n$ -dimensional simplex  $T_i$  or one of its  $(n-1)$ -dimensional face simplex.

Let  $V_h^{(i)}$  be the finite element space of order  $k$ :

$$V_h^{(i)} = \{v \in H^1(\Omega_i) \mid v|_T \in P_k(x_1, \dots, x_n) \quad \forall T \in \mathcal{T}_h\}. \quad (3.2)$$

Then we glue these finite element functions together:

$$V_h = \{v \in V_h^{(i)} \mid v(\varphi_i^{-1}(\mathbf{y})) = v(\varphi_j^{-1}(\mathbf{y})) \quad \forall \mathbf{y} \in \overline{M}_i \cap \overline{M}_j\}. \quad (3.3)$$

To be precise, a function of  $V_h$  is defined on multiple domains. For example, a nodal basis function  $b_k(\mathbf{x})$ , associated with a node  $\mathbf{y}_k \in \overline{M}_i \cap \overline{M}_j$ , is defined by, cf. Figure 3.1,

$$b_k(\mathbf{x}) = \begin{cases} b_k^{(i)}(\mathbf{x}), & \mathbf{x} \in \Omega_i, \\ b_k^{(j)}(\mathbf{x}), & \mathbf{x} \in \Omega_j, \end{cases} \\ b_k^{(i)}(\mathbf{x}) = \begin{cases} 1 & \mathbf{x} = \mathbf{x}_k^{(i)}, \\ 0 & \text{rest nodes of } \mathcal{T}_{(i),h}, \end{cases} \quad b_k^{(i)}(\mathbf{x}) \in V_h^{(i)}, \\ b_k^{(j)}(\mathbf{x}) = \begin{cases} 1 & \mathbf{x} = \mathbf{x}_k^{(j)}, \\ 0 & \text{rest nodes of } \mathcal{T}_{(j),h}, \end{cases} \quad b_k^{(j)}(\mathbf{x}) \in V_h^{(j)}.$$

In other words,  $b_k$  is defined piecewisely on  $\Omega_i$  and  $\Omega_j$ , and it is defined globally on  $M$  via two inverse mappings.

The finite element method, discretizing the nonoverlapping variational problem (2.3), is simply, solving  $u_h \in V_h$  such that

$$a(u_h, v_h) = (f, v_h) \quad \forall v_h \in V_h, \quad (3.4)$$

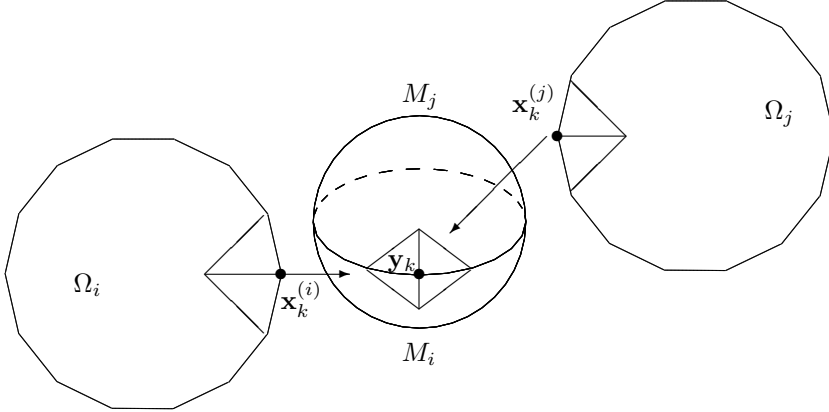


FIG. 3.1. Both  $\mathbf{x}_k^{(i)}$  and  $\mathbf{x}_k^{(j)}$  are mapped to  $\mathbf{y}_k$ ,  $\mathbf{y}_k = \phi_i(\mathbf{x}_k^{(i)}) = \phi_j(\mathbf{x}_k^{(j)})$ .

where the bilinear forms are defined by

$$\begin{aligned}
 a(u_h, v_h) &= \sum_i a_i(u_h, v_h) \quad \text{with} \\
 a_i(u_h, v_h) &= \int_{\Omega_i} \left( \sum_{\alpha, \beta=1}^n g_i^{\alpha\beta} \frac{\partial u_h}{\partial x_\alpha} \frac{\partial v_h}{\partial x_\beta} + b u_h v_h \right) \sqrt{G^{(i)}} d\mathbf{x}, \\
 (f, v_h) &= \sum_i \int_{\Omega_i} f v_h \sqrt{G^{(i)}} d\mathbf{x}.
 \end{aligned}$$

It is standard to prove the optimal order approximation of the finite element solution.

**THEOREM 3.1.** *Let  $\{\varphi_i\}$  be a set of nonoverlapping  $C^1$  coordinate charts on  $M$ , defined in (2.2). There is a unique solution  $u_h$  to the finite element equations (3.4). It approximates the solution to (2.1) at the optimal order,*

$$\|u - u_h \circ g^{-1}\|_{H^1(M)} \leq Ch^k \|u\|_{H^k(M)}$$

where the solution  $u \in C^\infty(M)$  is smooth on the compact manifold  $M$ .

*Proof.* Letting  $v_h = u_h$  (3.4), we found the coerciveness of the bilinear form

$$a(u_h, u_h) = \|u_h \circ g^{-1}\|_a^2 > 0$$

where  $\|\cdot\|_a$  denote the energy norm on Sobolev space  $H^1(M)$  on the manifold  $M$ . By Lax-Milgram theorem [6], (3.4) has a unique solution. By the orthogonal projection property,

$$\begin{aligned}
 \|u - u_h \circ g^{-1}\|_{H^1(M)}^2 &= Ca(u \circ g - u_h, u \circ g - u_h) \\
 &\leq C \|u \circ g - u_h\|_a \inf_{v \in V_h} \|u \circ g - v\|_a \\
 &\leq C \|u - u_h \circ g^{-1}\|_{H^1(M)} h^k \|u\|_{H^k(M)},
 \end{aligned}$$

where we apply (with a little adaptation) the Bramble-Hilbert lemma [6].  $\square$

However, the bilinear forms in (3.4) cannot be evaluated exactly by numerical quadratures if  $g_i^{\alpha\beta}$ ,  $\sqrt{G^{(i)}}$  and  $f(\varphi_i^{-1}(\mathbf{x}))$  are not polynomials. These are called variational crimes. The treatment is standard. That is, each chart  $\Omega_i$  is covered by

parametric elements of degree  $k$  such that the referencing mappings vanish at the Lobatto boundary nodes (not unique in high space dimension). Then, if the boundary of  $\Omega_i$  is piecewise smooth, we have the following bound on the perturbation due to boundary approximation (cf. Theorem 10.2.36 in [4]):

$$\left| \Omega_i \setminus \cup_{T \in \mathcal{T}_{(i),h}} T \right| \leq Ch^{k+1}, \quad (3.5)$$

where each  $T$  is an  $n$ -simplex with possibly one  $P_k$  face. Let us denote the parametric finite element space on the perturbed domains by  $\tilde{V}_h^{(i)}$ . The bilinear form approximation is also standard when choosing high enough order of quadratures (cf. Theorem 10.4.8 in [4]):

$$\sup_{\tilde{v} \in \tilde{V}_h^{(i)} \setminus \{0\}} \frac{|a_h(\tilde{u}_h, v) - a(u_h, \tilde{v})|}{\|\tilde{v}\|_{H^1(\Omega_i)}} \leq Ch^k \|u_h\|_{H^{k+1}(\Omega_i)}, \quad (3.6)$$

$$\sup_{\tilde{v} \in \tilde{V}_h^{(i)} \setminus \{0\}} \frac{|(f, v)_h - (f, \tilde{v})|}{\|\tilde{v}\|_{L^2(\Omega_i)}} \leq Ch^k \|f\|_{W_\infty^1(\Omega_i)}. \quad (3.7)$$

**COROLLARY 3.2.** *Suppose the domains  $\Omega_i$  and bilinear forms well approximated, i.e., (3.5)–(3.7) hold. Then the perturbed finite element solution converges at the optimal order too:*

$$\|u - \tilde{u}_h \circ \varphi^{-1}\|_{H^1(\tilde{M})} \leq Ch^k \|u\|_{H^k(M)}$$

where  $\tilde{u}_h \in \tilde{V}_h = \{\tilde{v}|_{\gamma_{ij}} = \tilde{v}|_{\gamma_{ji}} \mid v \in \tilde{V}_h^{(i)}\}$  such that

$$a_h(\tilde{u}_h, \tilde{v}) = (f, \tilde{v})_h \quad \forall \tilde{v} \in \tilde{V}_h.$$

□

Next, we introduce a finite element method for (2.1) with overlapping coordinate charts  $\{\varphi_i\}$  from (2.4). However, we have a very strong assumption that the grids on  $\Omega_i$  and  $\Omega_j$  are mapped to a same grid on the overlapping portion  $M_j \cap M_i$  on  $M$ , in (3.1). This assumption is to simplify the implementation techniques. If the grids on overlapping regions are non-matching, some nodal interpolation would be introduced to transfer functions from  $V_h^{(i)}$  to  $V_h^{(j)}$ . As usual, we do not consider numerical integration error. Otherwise the grid size  $h$  in Theorem 3.1 and Theorem 3.3 has to be sufficiently small, depending on the smoothness of  $M$  and the smoothness of coordinates  $\varphi_i$ . The finite element problem for the overlapping variational problem (2.5) is: find  $u_h \in V_h$  such that

$$a_i(u_h, v_h) = (f, v_h) \quad \forall v_h \in V_h^{(i)} \cap H_0^1(\Omega_i), \quad i = 1, \dots, K, \quad (3.8)$$

where  $a_i(\cdot, \cdot)$  is defined after (3.4).

**THEOREM 3.3.** *Let  $\{\varphi_i\}$  be a set of general, overlapping coordinate charts on  $M$ , defined in (2.4). There is a unique solution  $u_h$  to the finite element equations (3.8). It approximates the solution to (2.1) at the optimal order,*

$$\|u - u_h \circ \varphi^{-1}\|_{H^1(M)} \leq Ch^k \|u\|_{H^k(M)}$$

where the solution  $u \in C^\infty(M)$  is smooth on the compact manifold  $M$ .

*Proof.* The uniqueness of solution to (3.8) is proved exactly the same way as its continuous version (2.3), as we assume an grid matching (3.1) and no numerical quadrature error. By (3.8),

$$a(u \circ \varphi - u_h, v_h) = 0 \quad \forall v_h \in V_h^{(i)} \cap H_0^1(\Omega_i).$$

Due to interior overlapping (cf. Figure 2.1), for all nodal basis functions  $\phi_l$ ,

$$a(u \circ \varphi - u_h, \phi_l) = 0 \quad \forall \phi_l \in V_h.$$

That is, the  $a$ -orthogonal projection property is kept in (3.8). Thus

$$\begin{aligned} \|u - u_h \circ \varphi^{-1}\|_{H^1(M)}^2 &= Ca(u \circ \varphi - u_h, u \circ \varphi - u_h) \\ &\leq C\|u \circ \varphi - u_h\|_a \inf_{v \in V_h} \|u \circ \varphi - v\|_a \\ &\leq C\|u - u_h \circ \varphi^{-1}\|_{H^1(M)} h^k \|u\|_{H^k(M)}. \end{aligned}$$

□

**4. Numerical Experiments.** We perform three numerical tests on a sphere  $S^3$  in  $R^4$  with nonoverlapping charts or overlapping charts.

Let

$$M = S^3 = \{(y_1, y_2, y_3, y_4) \in R^4 \mid \sum y_i^2 = 1\}.$$

For nonoverlapping charts (2.2), we cut  $S^3$  along its equator  $\{y_4 = 0\}$  (see Figure 4.1), to get the upper hemisphere  $M_1$  and the lower hemisphere  $M_2$ . We use stereographic projection from the south pole  $(0, 0, 0, -1)$  and north pole  $(0, 0, 0, 1)$  to give  $M_1$  and  $M_2$  coordinate charts respectively, see Figure 4.2, where  $S$  and  $N$  are poles,  $P$  is on the sphere, and  $Q$  is on the  $R^{n-1}$ -plane, i.e.,  $R^3$ -hyperplane. We give the coordinates of  $Q$  to  $P$ , that is,

$$\varphi_i : P \mapsto Q, \quad \varphi_i : \Omega_i \rightarrow M_i. \quad (4.1)$$

Under these two coordinate charts, both  $\Omega_i$  for  $M_1$  and  $M_2$  are the 3-dimensional unit ball:

$$B_3 = \Omega_1 = \Omega_2 = \{(x_1, x_2, x_3) \in R^3 \mid x_1^2 + x_2^2 + x_3^2 \leq 1\}. \quad (4.2)$$

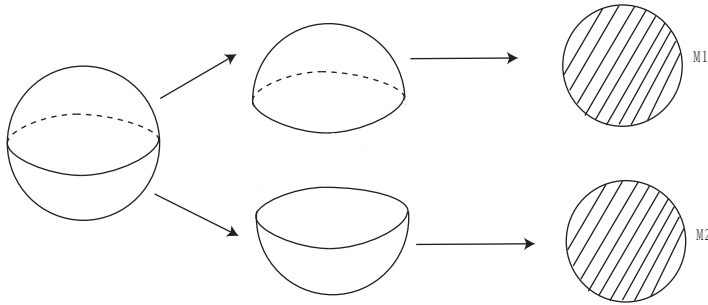
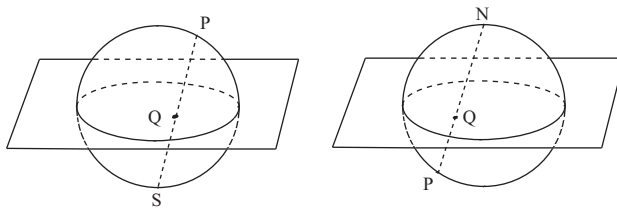
The grids on  $\Omega_i$  are standard multigrids [40], displayed in Figure 4.3.

The Riemannian metric for nonoverlapping (4.1) is

$$\frac{6}{(|\mathbf{x}|^2 + 1)^2} (dx_1 \otimes dx_1 \otimes dx_1 + dx_2 \otimes dx_2 \otimes dx_2 + dx_3 \otimes dx_3 \otimes dx_3). \quad (4.3)$$

The matrix  $(g_{\alpha,\beta})_{3 \times 3}$  is  $\frac{6}{(|\mathbf{x}|^2 + 1)^2} I_{3 \times 3}$ . This computation can be found in many textbooks of Riemannian Geometry, for example p. 33 in [22]. Thus we have, in both  $M_1$  and  $M_2$ ,

$$\Delta_S u = \frac{(x_1^2 + x_2^2 + x_3^2 + 1)^2}{6} \left( \sum_{i=1}^3 \frac{\partial^2 u}{\partial x_i^2} \right),$$

FIG. 4.1. Two nonoverlapping,  $C^1$ , charts for  $S^2$ , cf. (2.2).FIG. 4.2. Projections defining charts  $\varphi_1$  and  $\varphi_2$ .

$$\langle \nabla u, \nabla v \rangle = \frac{(x_1^2 + x_2^2 + x_3^2 + 1)^2}{6} \left( \sum_{i=1}^3 \frac{\partial u}{\partial x_i} \frac{\partial v}{\partial x_i} \right).$$

Let  $u$  be the height function of the sphere  $S^3$ , i.e.  $u = y_4$ . We solve equation (2.1), which becomes

$$-\Delta_S u + u = 4y_4. \quad (4.4)$$

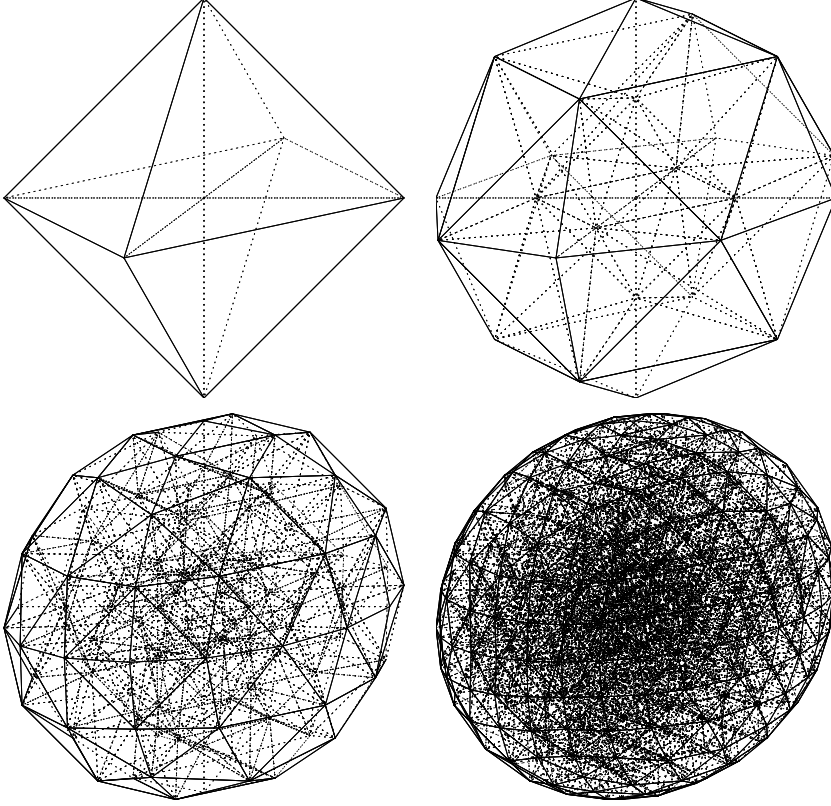
The solution is, on local coordinate charts,

$$u = \begin{cases} \frac{-x_1^2 - x_2^2 - x_3^2 + 1}{x_1^2 + x_2^2 + x_3^2 + 1} & \text{in } \Omega_1, \\ \frac{x_1^2 + x_2^2 + x_3^2 - 1}{x_1^2 + x_2^2 + x_3^2 + 1} & \text{in } \Omega_2. \end{cases} \quad (4.5)$$

We compute the problem with conforming  $P_1$  finite element, i.e.,  $k = 1$  in (3.3). First, we solve the global finite element directly by the conjugate gradient method. Due to a symmetry, only the top half problem is solved. The number of CG iterations are listed in the last column of Table 4.1. The convergence order is optimal, as predicted by Theorem 3.1. We note that we have a superconvergence in  $H^1$ -norm (see the seventh column of Table 4.1.) This is consistent to the work of [37] where a surface triangulation is applied to  $S^2$ . But the superconvergence is not proved in our paper here.

Next, we experiment the nonoverlapping domain decomposition method. We solve the finite element equations by the Robin-Robin nonoverlapping domain decomposition method [25, 9, 29, 30]. The coordinate charts for  $\partial M_1$  and  $\partial M_2$  are the unit sphere too, but in 3D, i.e.

$$S^2 = \{(x_1, x_2, x_3) \in R^3 \mid x_1^2 + x_2^2 + x_3^2 = 1\}.$$

FIG. 4.3. First 4 grids  $\mathcal{T}_{(i),h}$  on  $\Omega_i = B_3$ , cf. (4.2) and Table 4.1.TABLE 4.1  
The error (on  $M_1$ ) and order for (4.5).

	$\ I_h u - u_h\ _{L^2}$	$h^n$	$\ I_h u - u_h\ _{l^\infty}$	$h^n$	$ I_h u - u_h _{H^1}$	$h^n$	#CG
1	0.146367		0.400843		0.8016854972		2
2	0.0926666	0.7	0.217679	0.9	0.4451659853	0.8	4
3	0.028304	1.7	0.075876	1.5	0.1492563307	1.6	14
4	0.007812	1.9	0.023080	1.7	0.0483691271	1.6	36
5	0.002050	1.9	0.007179	1.7	0.0146292349	1.7	74
6	0.000522	2.0	0.002143	1.7	0.0042019146	1.8	150

The Riemannian metric matrix on the boundary integral is just  $I$ , the identity matrix. We get the iteration scheme as follows.

$$\begin{cases} A_i(u_i^n, v_i) + \lambda \int_{\gamma_{ij,h}} \pi_{ij} u_i^n \cdot \pi_{ij} v_i &= f_i(v_i) + \int_{\gamma_{ij,h}} r_{ij}^n \cdot \pi_{ij} v_i, \\ r_{ij}^{n+1} &= 2\lambda \cdot \pi_{ji} u_j^n - r_{ji}^n, \end{cases} \quad (4.6)$$

where  $i, j \in \{1, 2\}$ ,  $\pi_{ij}$  is the trace operator on  $\gamma_{ij}$ , and

$$A_i(u_i^n, v_i) = \int_{M_i} \left( \frac{2}{1 + |\mathbf{x}|^2} \sum_{j=1}^3 \frac{\partial u_i^n}{\partial x_j} \frac{\partial v_i}{\partial x_j} + \frac{8}{(|\mathbf{x}|^2 + 1)^3} u_i^n v_i \right) dx_1 dx_2 dx_3.$$

The boundary integral on  $\gamma_{ij,h}$  in (4.6) is computed via coordinate charts  $\Omega_i$  and  $\Omega_j$  (they are same when restricted to  $\gamma_{ij,h}$ ). The computational results are listed in Table 4.2. The number of nonoverlapping domain-decomposition iteration is listed in the last column. Here the iteration stops until the difference between last two iterates is less than  $10^{-5}$ .

TABLE 4.2  
The error and order by nonoverlapping DD, (4.5).

	$\ I_h u - u_h\ _{L^2}$	$h^n$	$\ I_h u - u_h\ _{l^\infty}$	$h^n$	$ I_h u - u_h _{H^1}$	$h^n$	#dd
1	0.204792		0.560723		1.1212842055		25
2	0.149337	0.5	0.363531	0.6	0.6285882667	0.8	25
3	0.057322	1.4	0.146772	1.3	0.2329487210	1.4	27
4	0.016304	1.8	0.047581	1.6	0.0701729023	1.7	27
5	0.004372	1.9	0.014098	1.8	0.0192478986	1.9	28
6	0.001178	1.9	0.004029	1.8	0.0050866812	1.9	28

As a final numerical test, we choose an overlapping set of charts for the manifold  $S^3$ . Since it would be difficult to make the piecewise charts  $C^1$  across the boundary, it is more practical to consider overlapping charts where the  $C^1$  continuity requirement is relaxed. In our test, we solve the problem (4.4) again with the solution (4.5). This time,  $\varphi_1$  and  $\varphi_2$  are defined the same way as (4.1), except they are extended further to the other half of sphere, shown in Figure 4.4. We choose  $\Omega_i$  to be a 3D sphere of radius 2 (not radius 1 as above):

$$\Omega_1 = \Omega_2 = \{(x_1, x_2, x_3) \in R^3 \mid x_1^2 + x_2^2 + x_3^2 \leq 2^2\}, \quad (4.7)$$

Then

$$M_1 = \left\{ (y_1, y_2, y_3, y_4) \in S^3 \mid y_4 \geq -\frac{3}{5} \right\},$$

$$M_2 = \left\{ (y_1, y_2, y_3, y_4) \in S^3 \mid y_4 \leq \frac{3}{5} \right\}.$$

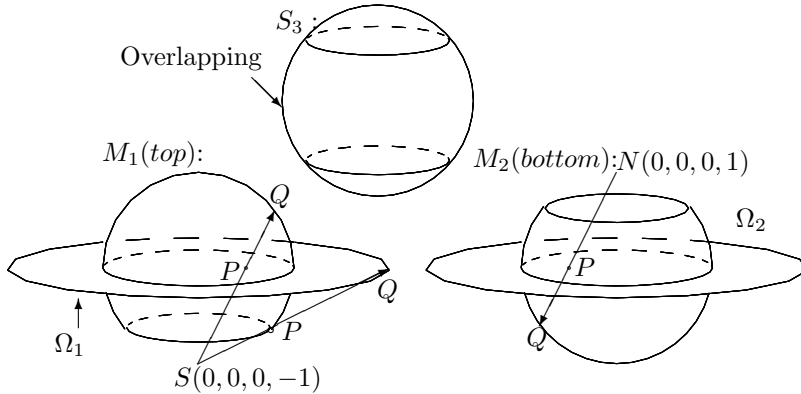


FIG. 4.4. Overlapping  $M_1$  &  $M_2$  ( $y_4 = \mp 3/5$ ), cf. (2.4) and (4.7).

We perform an overlapping domain decomposition method to solve (3.4). That

is, given  $u_{h,0}^{(2)} = 0$ , we find  $u_{h,i}^{(1)}$  and  $u_{h,i}^{(2)}$ ,  $i = 1, 2, \dots$ , by

$$\begin{cases} a_1(u_{h,i}^{(1)}, v_h) = (f, v_h) \quad \forall v_h \in V^{(1)}, \\ u_{h,i}^{(1)}|_{\partial M_1} = u_{h,i-1}^{(2)}|_{M_2^0}, \end{cases} \quad (4.8)$$

$$\begin{cases} a_2(u_{h,i}^{(2)}, v_h) = (f, v_h) \quad \forall v_h \in V^{(2)}, \\ u_{h,i}^{(2)}|_{\partial M_2} = u_{h,i}^{(1)}|_{M_1^0}. \end{cases} \quad (4.9)$$

Note that, due to overlapping, the boundary of  $M_1$  is in the interior of  $M_2$ , shown in Figure 4.4. Due to a big overlap, the domain decomposition converges very fast. Only 6 iterations are needed, to reach a  $10^{-5}$  difference. The numerical results are listed in Table 4.3. We note that, because the computation domain is twice as big as in last computation, a radius 2 ball in 3D, the errors in Table 4.3 are bigger than those listed in Tables 4.1 and 4.2. We note that the computation starts from grid 3 in Table 4.3. This is because we need the boundary data of  $u_{h,i}^{(1)}$  from the iterate  $u_{h,i-1}^{(2)}$  at some interior grid points, that is,

$$u_{h,i}^{(1)} \circ \varphi_1^{-1}|_{x_1^2+x_2^2+x_3^2=2^2} = u_{h,i-1}^{(2)} \circ \varphi_2^{-1}|_{x_1^2+x_2^2+x_3^2=(\frac{1}{2})^2}.$$

TABLE 4.3  
The error (bigger  $M_1$ ) and order by overlapping DD, (4.8).

	$\ I_h u - u_h\ _{L^2}$	$h^n$	$\ I_h u - u_h\ _{l^\infty}$	$h^n$	$\ I_h u - u_h\ _{H^1}$	$h^n$	#dd
3	0.493551		0.341005		0.9633354454		6
4	0.138991	1.8	0.127412	1.4	0.2774985855	1.8	6
5	0.038944	1.8	0.040861	1.6	0.0765976372	1.9	6
6	0.010936	1.8	0.012113	1.8	0.0207526761	1.9	6

## REFERENCES

- [1] D. N. Arnold, A. Mukherjee, L. Pouly, Adaptive finite elements and colliding black holes. Numerical analysis 1997 (Dundee), 1-15, Pitman Res. Notes Math. Ser., 380, Longman, Harlow, 1998.
- [2] E. Bansch, P. Morin and R. H. Nochetto, A finite element method for surface diffusion: the parametric case J. Comp. Physics, **203** (2005), 321343.
- [3] S. Bartels, Stability and convergence of finite element approximation schemes for harmonic maps, Math. Comp. **79** (2010), no. 271, 1263-1301.
- [4] S.C. Brenner and L. R. Scott, The Mathematical Theory of Finite Element methods, 3rd Ed., Springer, New York, 2008.
- [5] T. F. Chan and T. P. Mathew, Domain decomposition algorithms. In Acta Numerica 1994, 61-143, Cambridge University Press, 1994.
- [6] P. G. Ciarlet, The finite element method for elliptic problems, North-Holland, Amsterdam, 1978.
- [7] A. Demlow, Higher-order finite element methods and pointwise error estimates for elliptic problems on surfaces, SIAM J. Numer. Anal., **47** no. 2(2009), 805827.
- [8] A. Demlow and G. Dziuk, An adaptive finite element method for the Laplace-beltrami operator on implicitly defined surfaces, SIAM J. Numer. Anal., **45** no. 1(2007), 421442.
- [9] Q. Deng, An analysis for a nonoverlapping domain decomposition iterative procedure, SIAM J. Sci. Comput., **18** (1997), 1517-1525.
- [10] Q. Deng, A nonoverlapping domain decomposition method for nonconforming finite element problems, Comm. Pure Appl. Anal., **2** (2003), 295 -306.

- [11] T. A. Driscoll, A nonoverlapping domain decomposition method for Symm's equation for conformal mapping, *SIAM J. Numer. Anal.*, **36** No. 3 (1999), 922-934.
- [12] Q. Du and L. Ju, Finite volume methods on spheres and spherical centroidal Voronoi meshes, *SIAM J. Numer. Anal.* **43** No. 4(2005), 1673-1692.
- [13] G. Dziuk, Finite elements for the Beltrami operator on arbitrary surfaces. In *Partial differential equations and calculus of variations*, volume 1357 of *Lecture Notes in Math.*, 142155. Springer, Berlin, 1988.
- [14] G. Dziuk and C. M. Elliott, Finite elements on evolving surfaces, *IMA J. Num. Anal.* **27** (2007), 262-292.
- [15] M. J. Gander, and G. H. Golub, A nonoverlapping optimized Schwarz method which converges with an arbitrarily weak dependence on  $h$ , In *fourteenth international conference on domain decomposition methods*, 2002.
- [16] M. J. Gander, L. Halpern, and F. Nataf, Optimized Schwarz methods, In *Twelfth International Conference on Domain Decomposition Methods*, Chiba, Japan, 15-28, 2001.
- [17] C. F. Gauss, *Werke: herausgegeben von der Koniglichen Gesellschaft der Wissenschaften zu Gottingen*, 1838. Georg Olms, Verlag, New York, 1981.
- [18] E. Hopf, *Elementare Bemerkungen über die Lösungen partieller Differentialgleichungen zweiter Ordnung vom elliptischen Typus. (Elementary remarks concerning second order elliptic partial differential equations.)* Sitzungsber. d. Preuss. Akad. d. Wiss. 19 (1927), 147-152.
- [19] L. V. Hörmander, *Linear Partial Differential Operators*, **GMW 116**, Springer-Verlag, 1963.
- [20] J. Jost, *Riemannian Geometry and Geometric Analysis (4th edition ed.)*, Springer, 2005.
- [21] O. Korobkin, B. Aksoylu, M. Holst, E. Pazos and M. Tiglio, Solving the Einstein constraint equations on multi-block triangulations using finite element methods. *Classical Quantum Gravity* 26 (2009), no. 14, 145007, 28 pp.
- [22] J. M. Lee, *Riemannian Manifolds, An Introduction to Curvature*, **GTM 176**, Springer-Verlag, 1997.
- [23] P. L. Lions, On the Schwarz alternating method I, in the *First International Symposium on Domain Decomposition Methods for Partial Differential Equations*, 1988.
- [24] P. L. Lions, On the Schwarz alternating method II, in the *Second International Symposium on Domain Decomposition Methods for Partial Differential Equations*, 1989.
- [25] P. L. Lions, On the Schwarz alternating method III: a variant for nonoverlapping subdomains, In *Third International Symposium on Domain Decomposition Methods for Partial Differential Equations*, 1990.
- [26] J. Maes, A. Kunoth and A. Bultheel, BPX-type preconditioners for second and fourth order elliptic problems on the sphere. *SIAM J. Numer. Anal.* 45 (2007), no. 1, 206-222.
- [27] H.-S. Oh and I. Babuka, The method of auxiliary mapping for the finite element solutions of plane elasticity problems containing singularities, *J. of Comp. Physics*, **121** (1995), 193-212.
- [28] M. A. Olshanskii and A. Reusken, A finite element method for surface PDEs: matrix properties, *Numer. Math.*, **114** (2010), 491520.
- [29] L. Qin, and X. Xu, On a parallel Robin-type nonoverlapping domain decomposition method, *SIAM J. Numer. Anal.*, **44**(2006), 2539-2558.
- [30] L. Qin, and X. Xu, Optimized Schwarz methods with Robin transmission conditions for parabolic problems, *SIAM J. Sci. Comput.*, **31**(2008), 608-623.
- [31] A. Quarteroni, and A. Valli, *Domain decomposition methods for partial differential equations*, Oxford Science Publications, 1999.
- [32] G. de Rham, *Variétés Différentiables*, Hermann, Paris, 1973.
- [33] J.-F. Remacle, C. Geuzaine, G. Compré and E. Marchandise, High quality surface remeshing using harmonic maps, *Internat. J. Numer. Methods Engrg.* **83** (2010), no. 4, 403-425.
- [34] R. Schoen and S. T. Yau, On univalent harmonic maps between surfaces, *Invent. Math.*, **44** (1978), 265-278.
- [35] R. Schoen, and S. T. Yau, *Lectures on Differential Geometry*, Intl Pr of Boston Inc, 1994.
- [36] H. A. Schwarz, *Gesammelte Mathematische Abhandlungen*, volume 2, 133-143. Springer, Berlin, 1890. First published in *Vierteljahrsschrift der Naturforschenden Gesellschaft in Zürich*, volume 15, 272-286, 1870.
- [37] H. Wei, L. Chen and Y. Huang, Superconvergence and gradient recovery of linear finite elements for the Laplace-Beltrami operator on general surfaces, *SIAM J. Numer. Anal.*, **48** No. 5(2010), 1920-1943.
- [38] J.-J. Xu and H.-K. Zhao, An Eulerian formulation for solving partial differential equations along a moving interface *J. Scientific Computing*, **19**(2003), 573-594.
- [39] J. Xu and J. Zou, Some nonoverlapping domain decomposition methods, *SIAM Rev.*, **40** (1998), 857-914.
- [40] S. Zhang, Successive subdivisions of tetrahedra and multigrid methods on tetrahedral meshes,

- Houston J. of Math., **21** (1995), 541-556.
- [41] G. Zumbusch, Finite element, discontinuous Galerkin, and finite difference evolution schemes in spacetime. Classical Quantum Gravity 26 (2009), no. 17, 175011, 15 pp.